RESEARCH REPORT VTT-R-00784-23

Nuclear power plant ventilation system modelling with fire induced pressure data

Authors: Nikhil Verma

Confidentiality: VTT Public

Version: 07.12.2023

VTT

beyond the obvious

Report's title	
Nuclear power plant ventilation system modelling with fire induced pressure data	
Customer, contact person, address	**Order reference**
State Nuclear Waste Management Fund (VYR) SAFER2028 Programme	NA
Project name	**Project number/Short name**
Fire behaviour and safety of nuclear infrastructure (FASAANI)	135911/FASAANI
Author(s)	**Pages**
Nikhil Verma	20
Keywords	**Report identification code**
Nuclear Power Plant, Ventilation System, Fire, Compartment, FDS, Fire Dynamics Simulator	VTT-R-00784-23

Summary

A reliable computational model for a ventilation system and its interaction with fire-induced pressure in a nuclear power plant is crucial. This work has developed a systematic approach to build such a model. The method includes a procedure to discard noisy data and extract parameters from the fan curve, an equation to check the quality of the extracted fan parameters, and a tailored optimization technique. The developed method has been successfully tested and established the target pressure in the simulation with a -0.2% error. The method will be used in the 2024 task to reproduce the fire-ventilation interactions accurately, and the FDS implementation of the network model with estimated parameters will be validated using fire test data from OECD PRISME project. Overall, this systematic approach provides a reliable and efficient method to deal with limited data related to features and uncertainty in the parameters required to model complex ventilation systems.

Confidential data related to OECD PRISME project is excluded from this report.

Confidentiality	VTT Public

Espoo 7.12.2023

Written by	**Reviewed by**
Nikhil Verma, Research Scientist	Timo Korhonen Senior Scientist

VTT's contact address
Nikhil Verma, Kemistintie 3, Espoo, P.O. Box 1000, FI-02044 VTT, Finland (nikhil.verma@vtt.fi)

Distribution

SAFER2028, VTT

Approval

VTT TECHNICAL RESEARCH CENTRE OF FINLAND LTD

Date:	07.12.2023
Signature:	DocuSigned by: Marko Mäkipää EF95EB85E9804AC...
Name:	Marko Mäkipää
Title:	Research Team Leader, BA5503

Preface

This work has been carried out as a part of work package 1 of FASAANI project which is one of the projects in the SAFER2028. The work covers the task 1.1 of the project. Thanks are extended to the State Nuclear Waste Management Fund (VYR) and as well as other key organisations operating in the field of nuclear energy for funding the project work.

Espoo, 7.12.2023

Nikhil Verma

Contents

1. Introduction

In nuclear power plants, rooms are compartmented from each other through doors and walls, and at the same time are connected to each other through a ventilation network having different air inlets and outlets as shown in Figure 1. Such ventilation systems build pressure cascades to ensure confinement preventing the release of hazardous materials to the outside environment. With the pressure cascades in place with no general openings like windows or any other vents, rooms are generally quite sealed in terms of air leakages. The ventilation systems in place at times can regulate the pressure build up or release leading to a strong correlation between fire induced pressure and ventilation condition. In a fire, due to the gas expansion, pressure increases in a compartment, and ventilation conditions may get altered [Merci et al., 2016]. For example, smoke may enter the inlet branch and propagate against the nominal flow direction, thus reducing the flow of fresh air into the space which is needed by a fire to continue. After some time, the heat release rate of a fire starts to decrease due to the reduction of fresh air. The pressure in the room then decreases, and the flow of fresh air into the room starts again [Audouin et al., 2013]. The subsequent cyclic pattern affects the flow in the ventilation ducts and pressure in the room in conjunction with the prevailing heat release rate [Wahlqvist et al., 2013]. More is the heat release rate of a fire, more is the pressure developed in the room and vice versa. The flow of smoke through the inlet branch can lead to dangerous conditions if it enters other spaces served by the same system. Development of high pressure is also a concern [Li et al., 2020]. It has been noted in OECD/NEA PRISME campaign that pressure reached close to 3000 Pa in a compartment. As such pressure development and unwanted passage of smoke can endanger life safety and equipment safety [Prétrel et al., 2012], it becomes important to study the complex interaction of ventilation systems with fire to limit its undesirable effects.

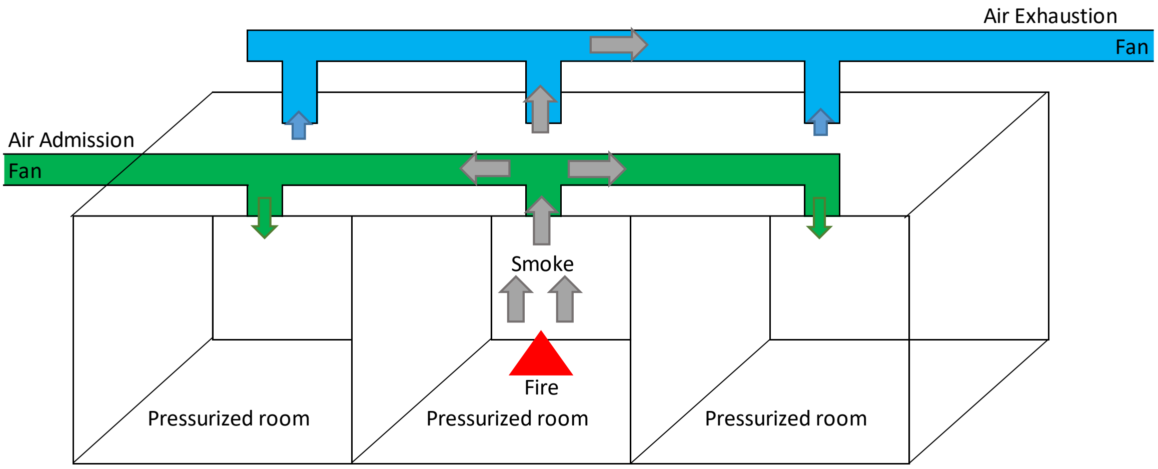

Figure 1. Example of compartmented rooms connected through a ventilation network in a nuclear power plant

Fire tests within the OECD/NEA PRISME campaigns have clearly shown the importance of compartment pressure, generating a significant track of scientific research, also outside the nuclear community [Hostikka et al., 2017]. Data recorded from a fire test in a room having an air inlet and outlet have shown the fire-induced pressure and ventilation coupling where when pressure was increasing in the compartment, the volumetric flow rate in the air inlet was decreasing and volumetric flow rate in the air outlet was increasing. All such data along with heat release rates of a fire are recorded with respect to time. Representative figures of pressure variation with time ($P(t)$) and inlet volumetric flow rates ($V_{inlet}(t)$) with time is shown in Figure 2.

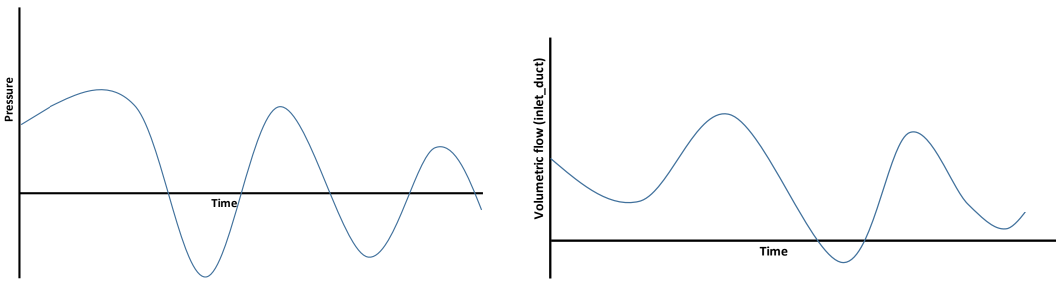

Figure 2. Representative figures of pressure variation with time and volumetric flow rates (inlet)

To carry out the CFD based simulations of such compartments, measured data like $P(t), V_{inlet}(t)$ and $V_{outlet}(t)$ (outlet volumetric flow rate) can be directly used as a boundary condition in the simulation of the very same experiment, but in order to generalize the data for other fire conditions, the network and its components need to be modelled [Wahlqvist et al., 2013; Li et al., 2021]. Parameters required to model a ventilation system are often found/extracted from the recorded data of network flow data, i.e., $V_{inlet}(t)$ and $V_{outlet}(t)$ along with the pressure in the room $P(t)$. Unfortunately, there is no standard method to analyse the network flow data and the data analysis is often hindered by noise (Figure 3, right). Manufacturers generally provide operating parameters for the ventilation fans, but the pressure range may not cover the pressures encountered in a fire situation. In addition, the lack of data concerning duct dimensions and network structure (elbows, bends, tees, valves etc.), loss coefficients, additional leakages etc. further exacerbate the problem [Brohez et al., 2020] to model such set-up in a CFD based software.

The main CFD software for the fire simulations is current Fire Dynamics Simulator (FDS) [McGrattan et al. 2023], which has a separate ventilation network solver (based on MELCOR, Sandia National Laboratories developed MELCOR, a computer code used by the US Nuclear Regulatory Commission to model severe accidents in nuclear power plants). A modelled network in FDS typically contains many simplifications, and the missing data are estimated through simulation trials [Li et al., 2021]. As fire behaviour is strongly coupled to the ventilation system performance (a case of a sealed compartment), it is of outmost importance to have reliable models of the design of complex ventilation systems through an established and proven method such that the method can be confidently used for other fire conditions and compartments. Next section explains the need to have an established and proven method such that hit-and-trail approach is minimized, and a systematic approach is adopted to make reliable models of ventilation systems in FDS wherein the expert judgments are not much needed, and results are reproducible following the outlined steps.

2. Goal

In this task (T1.1), the goal has been to develop a systematic method for finding unknown parameters for ventilation network model of complex ventilation system. With ventilation network model built, the overall aim has been to develop a target pressure in the simulation which is the steady pressure developed in the compartment during a real test just before the fire starts in the compartment using optimization technique. If such a steady pressure is able to be developed in a simulation by using estimated values for various ventilation parameters, then it is expected that when fire starts, the interaction of fire with the ventilation system can be modelled properly. For example, in the PRISME tests, the steady pressure (before fire starts) of the compartment has always been provided along with the volumetric flow rates in the ducts at that time and the leakage in the compartment. However, as fans propelling the flow in the ducts adjust its volumetric flow rates as per the pressure it experiences, using fixed volumetric flow rates for any inlet or outlet vents in FDS will not establish the target pressure in the room. Even if it is able to establish the target pressure (e.g., by hit-and-trails) in the room, it will not interact with fire and its resulting pressure, leading to unacceptable results in the end. For the cases with fixed volumetric flow rates, FDS will eventually establish an equilibrium pressure approximately based on ideal gas law which will not correspond to the HVAC system.

To carry out the task, the (real) test data concerning $P(t), V_{inlet}(t)$ and $V_{outlet}(t)$ is taken from one of the PRISME 3 tests in which fire was ignited in a two-room compartment connected through an open doorway. The compartment has one air inlet and one air outlet. The simulation model is built simplifying different complexities of a ventilation system and the missing parameters are estimated using data analysis, curve fitting, and optimization techniques. Special attention has been paid to the model stability and convergence, as well as the computational cost.

A specific problem which has been dealt with is related to the noise and fluctuations in the test pressure-volumetric flow data (fan curve). Such fan curves as depicted by blue line in Figure 3 (left image) provides two crucial values for fan operations, i.e., "V_{max}" and "P_{stall}". "V_{max}" is the point on the volumetric flow rate axis when the pressure against the fan is zero and "P_{stall}" is the pressure against the fan when it renders volumetric flow rate to zero. From such curve, it is clear that based on the different pressures, the volumetric flow rates in the fan ducts changes, and the fixed volumetric flow rates will not be able to produce such an interaction with the changing pressure. However, it has been challenging to fit a curve on such data as such comes with lot of noise as shown in Figure 3 (right image). Previous attempts have shown that such a noise can prevent one from finding a well-fitting analytical fan curves, and an attempt to develop an automatic procedure for parameter estimation will require a method to discard erroneous data and to filter out physical fluctuations that are real but unresolvable for the current model. It is to be noted that the pressure beyond P_{stall} can lead to reverse flow in ducts, and such pressure range and equivalent volumetric flow rates are typically not provided by fan manufactures.

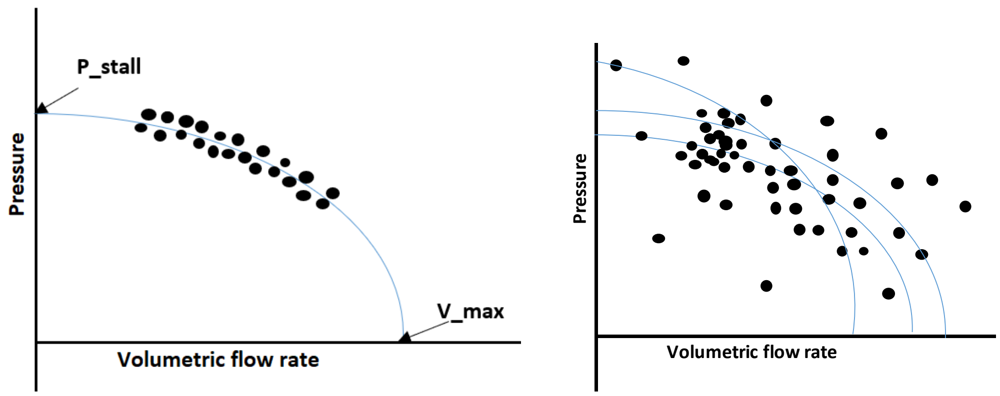

Figure 3. Representative pressure vs volumetric flow rate curve with noiseless data (left) and noisy data (right)

Moreover, once the fan parameters (“V_{max}” and “P_{stall}”) are determined, the duct network is required for simulations. To build duct network, one often at least needs duct’s features like length, cross-sectional area, loss coefficient (to account for pressure losses along the duct) along with the fan parameters. In most cases, values for such duct’s features are not known or estimated based on given information and are optimized for a stable pressure in the compartment.

Once, the ventilation network leading a stable pressure is established in the simulation, stable pressure has to be compared to the target pressure to check the quality of fan parameters extracted from the cleaned data. Based on the data quality and range of its coverage of various volumetric flow rates against pressures, it is possible that the extracted parameters are not able to produce the acceptable results. In such cases the fan parameters have to be optimized such that with iterations, the stable pressure converges to the target pressure. Next section explains the test case, computational domain for simulations, and underlying theory and equations for the pressure interaction with fans in the compartment.

3. Description

As mentioned before, a test case from PRISME 3 campaign has been taken in which a compartment has two rooms connected through a doorway (Figure 4). One room has an air inlet, and another room has an air outlet. A fire test was conducted in one of the room and data related to heat release rates, $P(t), V_{inlet}(t)$, and $V_{outlet}(t)$ was collected.

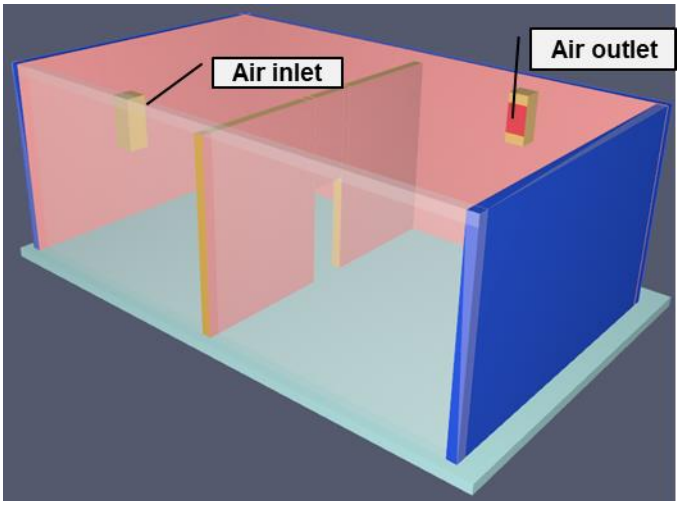

Figure 4. Computational set-up of a compartment from the PRISME 3 test case.

For data confidentiality, numerical values of data are not included in this report. However, following nomenclature has been used to denote the value of the variables of interest:

1. P_t = Target steady pressure established in the compartment (Pa)
2. P_s = Simulation steady pressure established in the compartment (Pa)
3. P = Random pressure in the compartment (Pa)
4. $P_{ambient}$ = Ambient pressure (Pa)
5. $P_{stall,in}$ = Stall pressure of the inlet fan (Pa)
6. $P_{stall,out}$ = Stall pressure of the outlet fan (Pa)
7. $m_{s,in}$ = Steady mass flow rate of the inlet fan or inlet duct (kg/s)
8. $m_{s,out}$ = Steady mass flow rate of the outlet fan or outlet duct (kg/s)
9. $m_{s,leak}$ = Steady mass flow rate of leakage (kg/s)
10. $V_{s,leak}$ = Steady volumetric flow rate of leakage (m^3/s)
11. $V_{s,in}$ = Steady volumetric flow rate of the inlet fan or inlet duct (m^3/s)
12. $V_{s,out}$ = Steady volumetric flow rate of the outlet fan or outlet duct (m^3/s)
13. $V_{max,in}$ = Volumetric flow rate of the inlet fan when pressure is zero in the compartment (m^3/s)
14. $V_{max,out}$ = Volumetric flow rate of the outlet fan when pressure is zero in the compartment (m^3/s)
15. $A_{L,ref}$ = Reference leakage area in the compartment (m^2)
16. A_L = Leakage area of the compartment (m^2)
17. ΔP_{ref} = Reference pressure to be established in the compartment (Pa) at which $A_{L,ref}$ is determined
18. ΔP = Pressure difference between the adjacent compartments or over pressure with respect to the atmospheric pressure at a given time (Pa)
19. C_d = Discharge coefficient for leakage (unitless, taken as 1)
20. ρ_∞ = Ambient density of air (kg/m^3)
21. ρ_{gas} = Density of gas (kg/m^3)
22. V_{leak} = Volumetric flow rate through leakage (m^3/s)
23. n = Exponent of the leakage pressure (unitless)

24. $v_{in\ or\ out}$ = volumetric flow rate of fan at a given ΔP (m^3/s)
25. A_{duct}= Cross-sectional area of the duct (m^2)
26. K= loss coefficient of the duct (unitless)
27. u = Mean velocity in a duct (m/s)
28. ΔP_{nodes} = Pressure difference between two nodes in a duct (Pa)
29. T = Tuning factor (unitless)
30. M = Molar mass of air
31. T_{emp} = Temperature of air (K)
32. R = Gas constant (J/K.mol)

In all the simulations, CFD based Fire Dynamics Simulator (FDS) software (version 6.8.0) has been used [McGrattan et al., 2023]. The computational domain has a single uniform mesh of 0.2 m with the compartment connected to the outside environment with ventilation ducts and leakages. Pressure zone leakage concept of the FDS software has been used in which the V_{leak} is calculated as follows:

$$V_{leak} = C_d A_L sign(\Delta P) \left(\frac{2|\Delta P|}{\rho_\infty}\right)^{0.5}$$ --equation 1

A_L is calculated as follows:

$$A_L = A_{L,ref} \left(\frac{|\Delta P|}{\Delta P_{ref}}\right)^{n-0.5}$$ ---equation 2

$n, \Delta P_{ref}, and\ A_{L,ref}$ for equation 2 has been determined from the experimental data of PRISME3 test, and $A_L$dependent on $|\Delta P|$ is used in the equation 1 to calculate the volumetric flow rate of leakage by FDS. Equation 2 clearly indicates that for $n > 0.5$, the area of leakage increases with increase in the pressure in the compartment which has been the case under this study.

The volumetric flow rate of a fan as a function of ΔP (other variables in the equation 3 are constant) in FDS software, e.g., for inlet fan, is given by:

$$v_{in} = V_{max,in}\ \mathrm{sign}(\Delta \mathrm{P}_{stall,in} - \Delta P) \sqrt{\frac{|\Delta P - \Delta \mathrm{P}_{stall,in}|}{\Delta \mathrm{P}_{stall,in}}}$$ ---equation 3

It can be noted from the equation 3, if rearranged is quadratic in nature (see equation 5), and that any change in ΔP affects the volumetric flow rate of the fan in conjunction with the pre-determined values of P_{stall} and V_{max} determined from the fan curve or related data. Thus, it is clear that the quality of P_{stall} and V_{max} estimated from the fan curve or related data will affect the volumetric flow rate of the fans. Next section explains how data analysis, curve fitting, and how ventilation ducts are built and optimized to achieve a target pressure in the simulation. Data analysis and curve fitting has been done using Python 3.10.9 (packaged by Anaconda, Inc.).

4. Methodology and Results

Data from the test were provided for $P(t), V_{inlet}(t)$, and $V_{outlet}(t)$ as shown in the Table 1 for the whole duration of the test.

Table 1. Tabular representation of the data used from the test.

Time_s	$P(t), Pa$	$V_{inlet}(t), m^3s^{-1}$	$V_{outlet}(t), m^3s^{-1}$
t_0	P_0	V_{in}_0	V_{out}_0
t_1	P_1	V_{in}_1	V_{out}_1
t_2	P_2	V_{in}_2	V_{out}_2
t_3	P_3	V_{in}_3	V_{out}_3
…	…	…	…
t_n-2	P_n-2	V_{in}_n-2	V_{out}_n-2
t_n-1	P_n-1	V_{in}_n-1	V_{out}_n-1
t_n	P_n	V_{in}_n	V_{out}_n

Before carrying out data analysis, data related to $P(t), V_{inlet}(t)$, and $V_{outlet}(t)$ were normalized using Min-max normalization technique to see the fluctuations in them on same scale. A variable is scaled between 0 and 1 when Min-max normalization is done as follows:

$$Variable_{scaled} = \frac{Variable_{value} - Variable_{minimum}}{Variable_{maximum} - Variable_{minimum}} \text{ --equation 4}$$

Percentage change in the scaled values of $P(t), V_{inlet}(t)$, and $V_{outlet}(t)$ clearly showed that the physical fluctuations in the pressure readings were more than the volumetric flow rates in ducts (Figure 5). Thus, values of $P(t)$ were chosen to spot the timestamps where there were high fluctuations leading to noisy data.

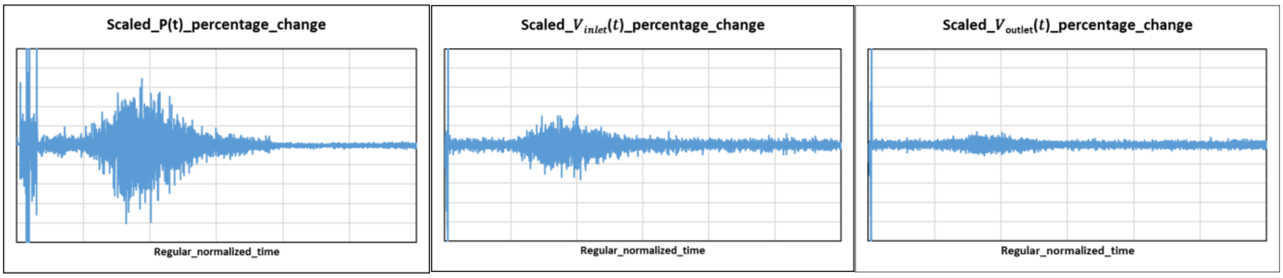

Figure 5. Percentage change in normalized values of $P(t), V_{inlet}(t)$, and $V_{outlet}(t)$.

Timestamps where there were high relative (not absolute) fluctuations (noisy data) in the $P(t)$ readings were automatically found using a technique based on coefficient of variations (a measure of variability). Coefficient of variation simply indicates the level of dispersion around the mean value. Higher the coefficient of variation, higher the dispersion around the mean value. For any time-interval for the case under study, coefficient of variation was computed by dividing standard deviation by mean value obtained for a variable over a chosen time interval. In case of zero mean value, the resulting NaN (Not a Number) has to be dealt separately based on the data using various available data wrangling techniques. However, no zero mean value was found in this study leading to any NaN value.

Coefficient of variations were computed for each time interval of 10 seconds (10 s averaging for finding the mean value and standard deviation) for $P(t)$, and outliers of values of coefficient of variations based on the concept of interquartile-range's outliers were selected to spot the respective timestamps (time intervals). All the values of $P(t), Vinlet(t)$, and $V_{outlet}(t)$ pertaining to those spotted timestamps (time interval) were discarded from the dataset resulting in the data set relatively less of noise and fluctuations. *Figure 6* shows the min-max normalized raw data, 10 s averaged normalized raw data, coefficient of variation, and selected datapoints (after dropping the spotted timestamps).

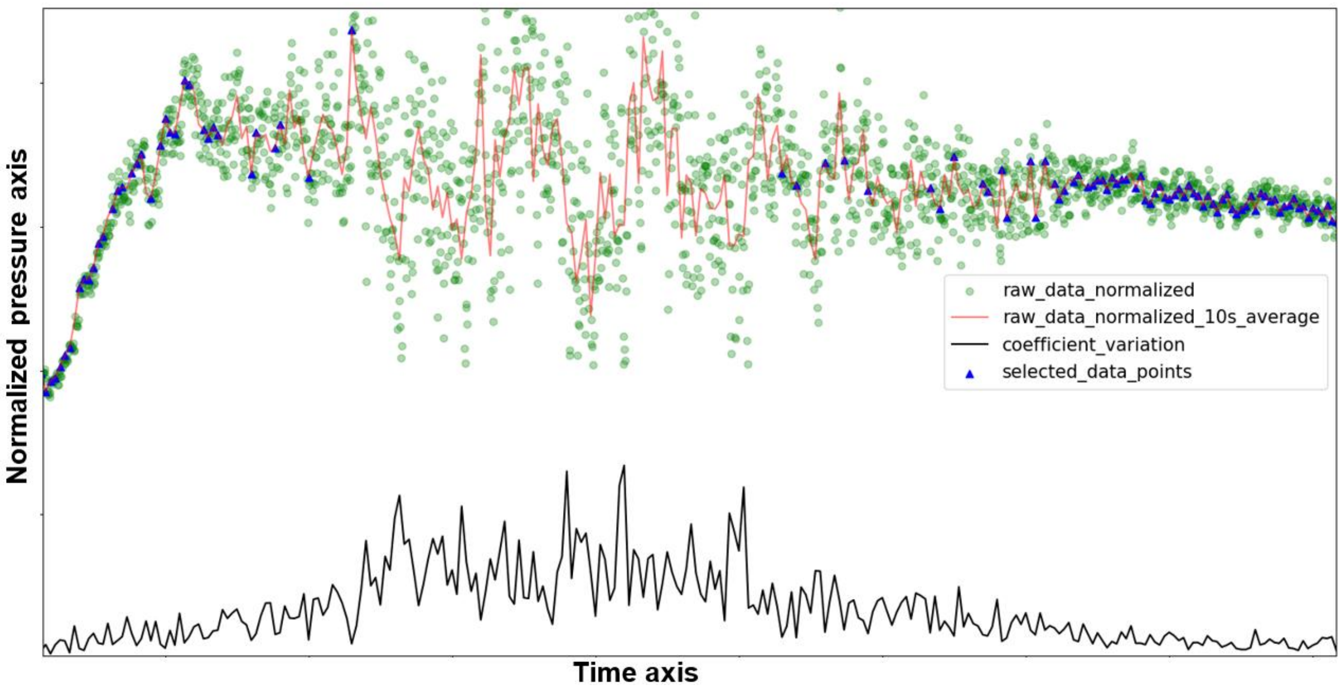

Figure 6. Data related to $P(t)$: normalized raw data, 10 s averaged normalized raw data, coefficient of variation, and selected datapoints.

The selected data is now ready for quadratic curve fitting to extract the "V_{max}" and "P_{stall}" for the fan where the curve intersects with the axis as shown in Figure 3. The general form of quadratic function where pressure as a function of volumetric flow rate of a fan is given as $P(v) = av^2 + bv + c$ (a, b, and c are constant) is not suitable for the fan model to be used in FDS. If equation 3 is rearranged for the case of no reverse flow in ducts which is the initial case in consideration when steady pressure is established in the compartment, we get

$\mathrm{P}(v) = -\frac{P_{stall}}{V_{max}^2} v^2 + P_{stall}$ --equation 5

which can be represented as $\mathrm{P}(v) = av^2 + \mathrm{b}$ where $a = -\frac{P_{stall}}{V_{max}^2}$ and $b = P_{stall}$. To fit such specific quadratic curve, SKLEARN library of python programming language was used from which polynomial regression fitted the required curve to the data and gave the values of a and b. A snippet of the code is shown in Figure 7.

```
from sklearn.preprocessing import PolynomialFeatures
from sklearn.linear_model import LinearRegression
from sklearn.metrics import mean_squared_error
```

```
poly= PolynomialFeatures(degree=(2, 2), include_bias=False)
x_poly= poly.fit_transform(x_1)
#print(x_poly)
```

```
Pressure(Volmetric_flow_rate) = xxxx )(Volmetric_flow_rate^2) + xxxx
R-square = 0.99
Root Mean Square Error = XXXX
MAX_PRESSURE_Stall= xxxx Pa
MAX_FLOW= xxxx m3/s
```

Figure 7. Snippet of python code to fit the quadratic curve to the data

Thus, the values for $P_{stall,in}$, $P_{stall,out}$, $V_{max,in}$, and $V_{max,out}$ were extracted from the data. To check the quality of the extracted values, an equation involving such variables of interest was derived based on the laws of conservation of mass for the compartment as a control volume for steady pressure condition. For compartment being considered as a control volume, the following mass rate balance is applicable (density of air is assumed to be constant as the temperature inside the compartment is nearly same as the ambient condition):

$$\begin{bmatrix} time\ rate\ of\ change \\ of\ mass\ contained \\ within\ the\ control \\ volume\ at\ time\ t \end{bmatrix} = \begin{bmatrix} time\ rate\ of\ flow \\ of\ mass\ into\ the \\ control\ volume \end{bmatrix} - \begin{bmatrix} time\ rate\ of\ flow \\ of\ mass\ out\ of \\ the\ control\ volume \end{bmatrix} \text{------equation 6}$$

During the steady operational pressure, the net rate of mass transfer into the control volume accompanying mass flow should equate to zero. Thus, we get:

$$\begin{bmatrix} time\ rate\ of\ flow \\ of\ mass\ into\ the \\ control\ volume \end{bmatrix} = \begin{bmatrix} time\ rate\ of\ flow \\ of\ mass\ out\ of \\ the\ control\ volume \end{bmatrix} \text{------equation 7}$$

Such mass transfers are done by the two fans, and leakage through their volumetric flow rates. The time rate of flow of mass is the product of density and volumetric flow rate of gas (air here). The density of the gas for various volumetric flow rates can be calculated using ideal gas equation (equation 8a):

$$\rho_{gas} = \frac{PM}{R\,T_{emp}} \text{------equation 8a}$$

Before proceeding further, it is important here to note that as the pressure difference and the temperature difference between the compartment and ambient condition (we have ambient node) is negligible, the density of the gas is assumed to be constant and equal to ρ_∞ for various volumetric flow rates. However, in the cases where the gas density in the compartment is considerably different from the outside compartment conditions, then ideal gas equation should be used to compute the gas density to account for the resulting differences. Such conditions prevail when fire in the compartment changes the gas temperature and increases the pressure manifolds based on the prevailing ventilation and leakage condition. Since we do not have fire in the present case and density of gas in the compartment is fairly assumed to same as the ambient condition, we can use the following equations for various mass flow rates:

$$\frac{dm_{s,in}}{dt} = \rho_\infty V_{s,in} \text{------equation 8b}$$

$$\frac{dm_{s,out}}{dt} = \rho_\infty V_{s,out}$$ --------equation 8c

$$\frac{dm_{s,leak}}{dt} = \rho_\infty V_{s,leak}$$ --------equation 8d

Equating equations 8b, 8c, and 8d for mass flow rate balance, we get

$$\rho_\infty V_{s,in} = \rho_\infty V_{s,out} \pm \rho_\infty V_{s,leak}$$

$$=> V_{s,in} = V_{s,out} \pm V_{s,leak}$$ --------equation 9

where, $V_{s,leak}$ is taken into account based on the development of under pressure or over pressure in the compartment (under pressure or over pressure determines the direction of leakage and hence the $\pm$ sign).

Using equation 3 for volumetric flow rate in equation 9 for steady operation pressure condition, we get

$$V_{max,in}\,\text{sign}(\Delta P_{stall,in} - \Delta P)\sqrt{\frac{|\Delta P - \Delta P_{stall,in}|}{\Delta P_{stall,in}}} = V_{max,out}\,\text{sign}(\Delta P_{stall,out} - \Delta P)\sqrt{\frac{|\Delta P - \Delta P_{stall,out}|}{\Delta P_{stall,out}}} \pm V_{s,leak}$$ --------equation 10

where, $\Delta P = P_t$ which is already known. Moreover, the rate of volumetric flow rate of leakage has been calculated from the provided data.

It is clear from the equation 10 that the extracted values of $P_{stall,in}$, $P_{stall,out}$, $V_{max,in}$, and $V_{max,out}$ from the data can be checked if they ensure mass flow rate balance or not before proceeding further. On checking, it was found that the value of $P_{stall,out}$ was underestimated for which the first correction was made. The prime reason suspected of underestimation is that the datapoints for the outlet vent might not have covered a satisfactory range of volumetric flow rate change with pressure which influenced the quadratic curve to intersect the pressure axis at lower value. Given the fact that the pattern of pressure-volume datapoints is comparatively complex and different for outlet vent compared to the inlet vent, such issues for the outlet vents are not surprising. For reference, one can check figure 8.7 and figure 8.8 in [Merci et al., 2016] which exemplifies such differences and complexities in outlet vent data. The first corrected value of $P_{stall,out}$ along with the extracted values $P_{stall,in}$, $P_{stall,out}$, $V_{max,in}$ was used for building ventilation duct model and duct length optimization based on the calculated total loss coefficient (explained below, Figure 8), and 0th iteration to optimize pressure build up in the compartment (explained below, Figure 10).

Next step involves building ventilation duct model in FDS software by incorporating various features of ducts like length, cross-sectional area, loss coefficient (to account for pressure losses along the duct) along with the fan parameters. It is important to note here that neither the duct length, cross-sectional area, loss coefficient, and details about its intermediate branching were known for the modelling.

The ventilation duct model was made based on the assumption that there is a single duct each for both vents starting at the ambient condition (ambient node) and ending in the compartment (vent node). To support such simplification in the lack of data of duct features, cross-sectional area of duct was taken same as the area of the respective vent in the compartment and loss coefficient was calculated using the equation 11 which uses the assumed cross-sectional area of the duct into the calculation of velocity in the duct (equation 12) and pressure difference between the ambient node and vent node in the compartment (equation 13):

$$K = \frac{2(\Delta P_{nodes})}{\rho_\infty u^2}$$ --------equation 11

$$u = \frac{V_s}{A}$$ --------equation 12

$\Delta P_{nodes} = P_t - P_{ambient}$ --equation 13

The data of volumetric flow rate, V_s, in the duct was provided. The single feature, i.e., K calculates the equivalent loss coefficient accounting for our assumptions for single duct connecting the compartment vent directly to the ambient node and chosen cross-sectional area for the duct. Based on our simplification of duct setup it is important here to note that K here stands for total loss coefficient which accounts for fitting loses in the duct (losses due to bend, elbows, reduction, or expansion etc.) and losses due to wall friction (duct roughness). To implement such simplification in FDS, the simulation parameter “ROUGHNESS” is left unset (not considered) in all the simulations so that the only calculated K accounts for the total losses in the duct through FDS parameter “LOSS” (interested reader can refer annexure A to check the insensitiveness of results when different roughness value are incorporated in the simulation). However, such simplifications will not lead to acceptable results unless the length feature is also optimized to establish a converging/steady pressure in the room.

To unilaterally optimize the duct length for the calculated total loss coefficient, the first corrected value of $P_{stall,out}$ along with the extracted values $P_{stall,in}$, $P_{stall,out}$, $V_{max,in}$ was used in simulation for various duct lengths, and at duct length L8 pressure converged to steady value (Figure 8). However, the steady value was 30% higher than the target pressure in the simulation.

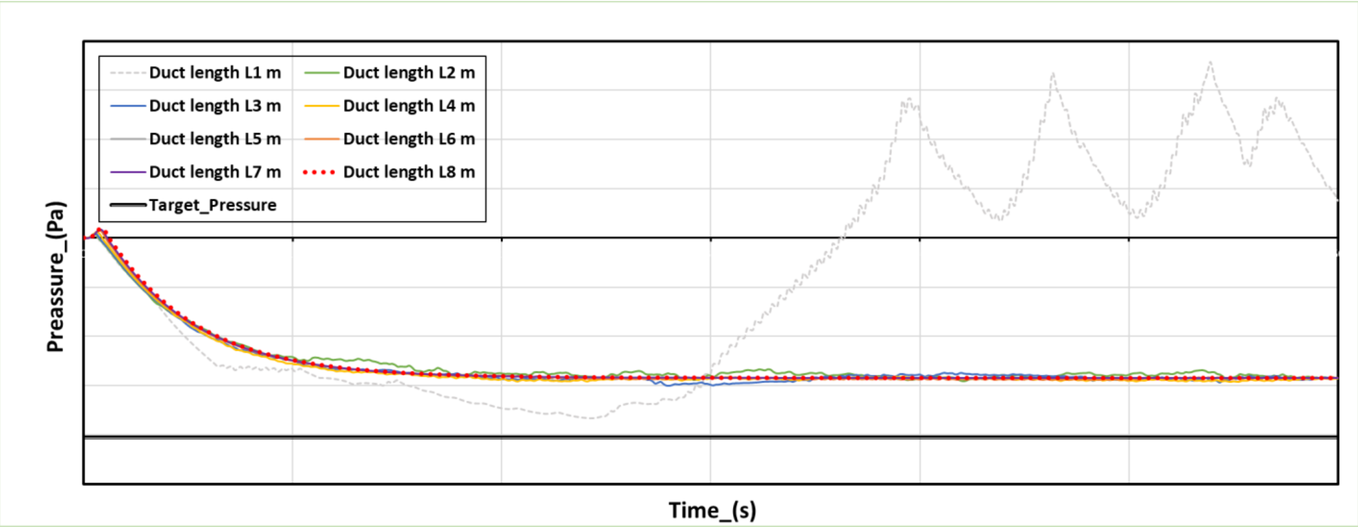

Figure 8. Duct length optimization to reach a steady pressure condition.

As the established pressure was 30% higher than the target pressure, it was clear that the values of parameters of either inlet fan or outlet fan (or both at the same time) needed optimization so that the simulation pressure converge to the target pressure, i.e., $P_s \rightarrow P_t$ in the simulation. Under the present case, value of parameters of outlet fan was chosen, and its $V_{max,out}$ and subsequent value of $P_{stall,out}$ calculated from the equation 10 was optimized to converge to the P_t.

To converge to the P_t, iterative process using the technique based on non-adaptive optimization (such optimizations have fixed learning rate) was followed. For the non-adaptive optimization, an objective function is defined which has to be minimized. In this case, the objective function, $f(P_s)$, is defined as follows:

$f(P_s) = \frac{100(P_t - P_s)\%}{P_t}$ --equation 11

Such percentage difference expressed by the objective function was multiplied by a tuning factor (T) which determined how fast the objective function was minimized. Tuning factor draws analogy to the Hyper-parameter concept in machine learning which defines learning rate for model to learn and optimize. In this study, the tunning factor is taken as 0.02. These are external configuration variables that has to be chosen by the user before optimization is carried out. It has nothing to do with the physical parameters of the simulations.

Starting with the first corrected values $P_{stall,out}$ along with the extracted values of $P_{stall,in}$, $P_{stall,out}$, $V_{max,in}$, $f(P_s)$ was first calculated. If $f(P_s)$ is high (means error is high and unacceptable) then it needs to be reduced. In such case, $f(P_s)$ is multiplied by T to get $f(P_s)T = 0.02f(P_s)$. For next iteration (simulation), $V_{max,out}$ is reduced by $0.02f(P_s)$% and corresponding $P_{stall,out}$ is calculated from the equation 10 and feed into the simulation. If the resulting $f(P_s)$ after iteration is still high and not acceptable then for next iteration (simulation), $V_{max,out}$ is again decreased by $0.02f(P_s)$% and corresponding $P_{stall,out}$ is calculated from the equation 10 and feed into the simulation, and the process is repeated until we get the acceptable $f(P_s)$.

For the given case, by the end of 13th iteration, pressure converged to the target pressure shown in Figure 10, Figure 10 and Table 2 with final error of -0.2%. Hence, target steady operational pressure was established in the simulation.

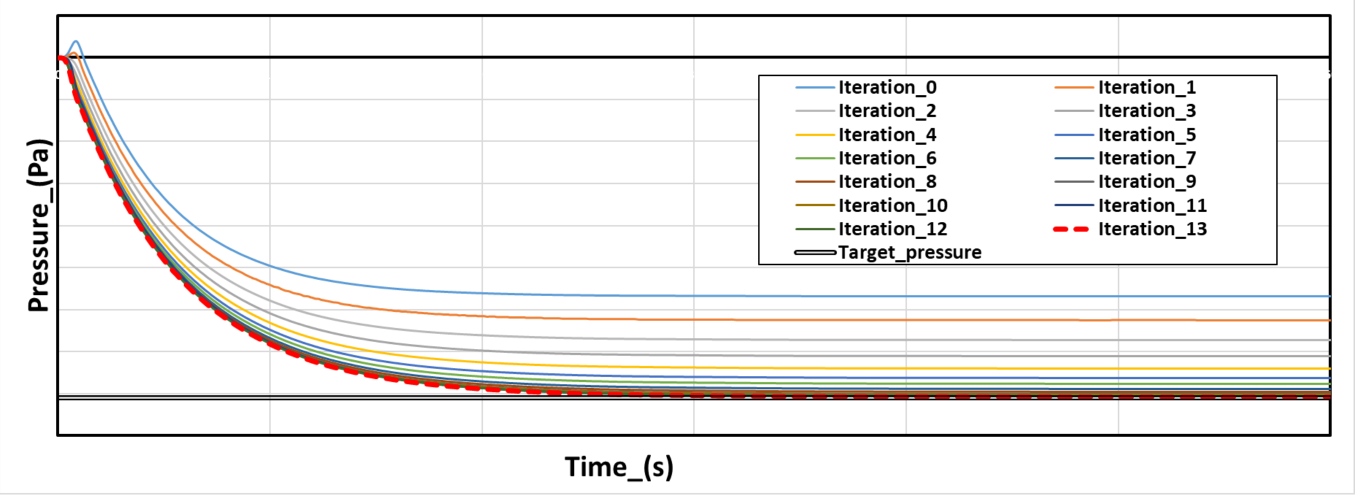

Figure 9. Pressure development with various iterations

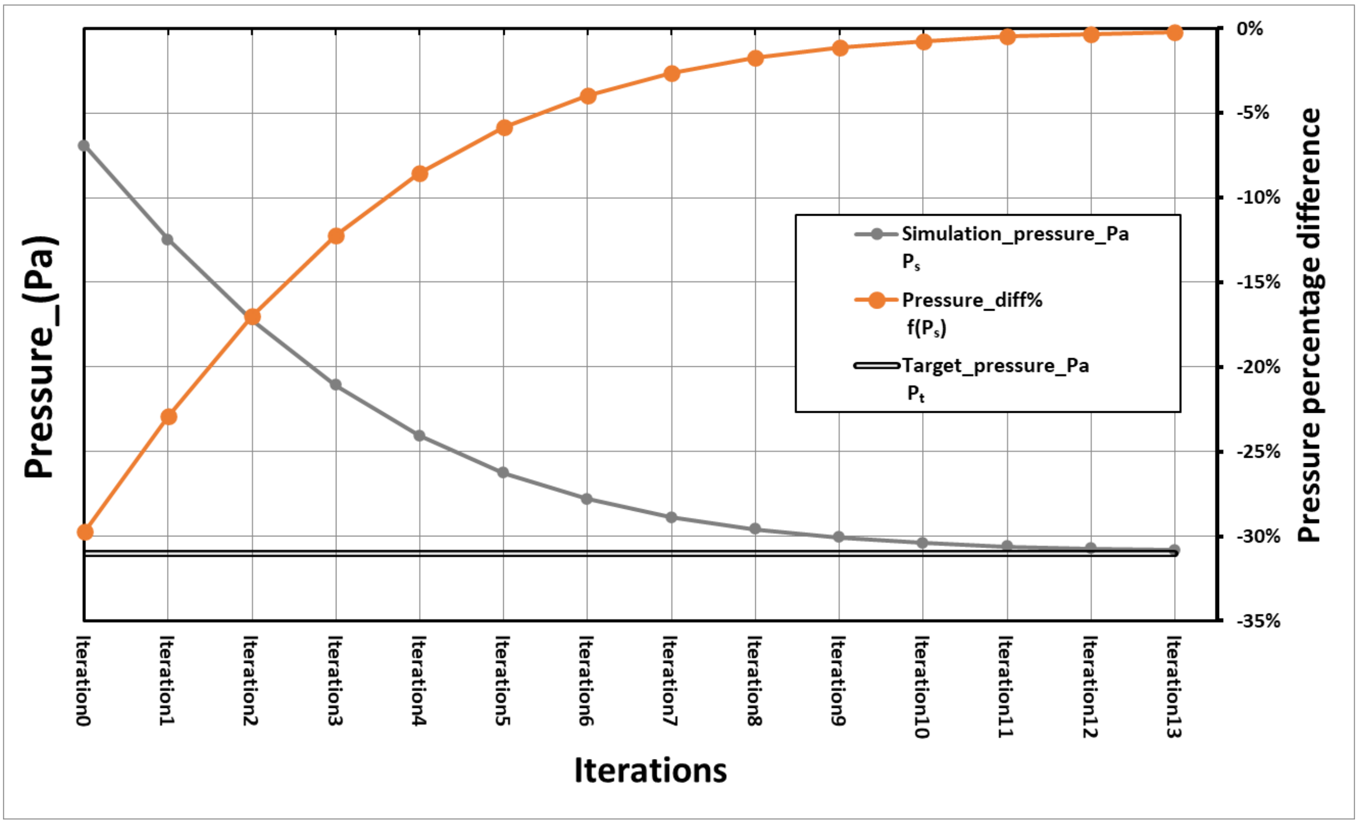

Figure 10. Pressure convergence and minimization of $f(P_s)$ with various iterations

Table 2. Iteration table and percentage change in $f(P_s)$ and $V_{max,out}$ with each iteration

	Target_pressure_Pa P_t	Simulation_pressure_Pa P_s	Pressure_diff% $f(P_s)$	%_Change_in_Outlet_V_max_for_next_iteration Vmax,out	Outlet_V_max_m3_per_s Vmax,out	Outlet_P_stall_Pa Pstall,out
Iteration0			-29.7%	0.594321%		
Iteration1			-22.9%	0.457531%		
Iteration2			-17.0%	0.340247%		
Iteration3			-12.2%	0.244691%		
Iteration4			-8.6%	0.171111%		
Iteration5			-5.9%	0.117037%		
Iteration6			-3.9%	0.078765%		
Iteration7	Confidential data!		-2.6%	0.052346%	Confidential data!	
Iteration8			-1.7%	0.034815%		
Iteration9			-1.1%	0.022716%		
Iteration10			-0.8%	0.015062%		
Iteration11			-0.5%	0.009630%		
Iteration12			-0.3%	0.006420%		
Iteration13			-0.2%	0.003951%		

5. Conclusions

A reliable computational model must be built to model a ventilation system and its complex interaction with fire-induced pressure in a nuclear power plant's compartment. The lack of a standard method to deal with limited data related to features and uncertainty in the parameters required to model such systems created a need to develop a systematic approach to address the problem. This work has developed a systematic method for finding unknown parameters for the ventilation network model of a complex ventilation system and its optimization to reach a target pressure in the simulation.

The method includes a procedure to discard the noisy data, parameter extraction from the fan curve, a mass flow rate balance equation to check the quality of the extracted fan parameters, and a tailored optimization technique suiting the problem of pressure optimization for the type of case under consideration. Overall, with the application of the method, target pressure in the simulation was established with a -0.2% error, which highlights the success of the developed method.

The developed method will be used in the 2024 task to check how satisfactorily it will lead to models that correctly reproduce the fire-ventilation interactions and safety–critical coupling features. In practice, we will validate the FDS implementation of the network model with estimated parameters using fire test data from OECD PRISME. Specific steps of the task will be to check the response of the estimated quadratic fan parameters with fire conditions and to quantify the sensitivity of the predicted over-pressures and flow anomalies (reverse flows causing possible hazards) on the ventilation modelling choices and simplifications.

References

Audouin L., Rigollet L., Prétrel H., Le Saux W., Röwekamp M., OECD PRISME project: Fires in confined and ventilated nuclear-type multi-compartments - Overview and main experimental results, Fire Safety Journal, Volume 62, Part B, 2013, Pages 80-101, ISSN 0379-7112, https://doi.org/10.1016/j.firesaf.2013.07.008

Brohez S., Caravita I., Fire induced pressure in airthigh houses: Experiments and FDS validation, Fire Safety Journal, Volume 114, 2020, 103008, ISSN 0379-7112, https://doi.org/10.1016/j.firesaf.2020.103008

Hostikka, S., Kallada Janardhan, R., Riaz, U., Sikanen, T. Fire-induced pressure and smoke spreading in mechanically ventilated buildings with air-tight envelopes. Fire Safety Journal, 91:380-388. 2017. https://doi.org/10.1016/j.firesaf.2017.04.006

Li J., Beji T., Brohez S., Merci B., CFD study of fire-induced pressure variation in a mechanically-ventilated air-tight compartment, Fire Safety Journal, Volume 115, 2020, 103012, ISSN 0379-7112, https://doi.org/10.1016/j.firesaf.2020.103012

Li J., Prétrel H., Suard S., Beji T, Merci B., Experimental study on the effect of mechanical ventilation conditions and fire dynamics on the pressure evolution in an air-tight compartment, Fire Safety Journal, Volume 125, 2021, 103426, ISSN 0379-7112, https://doi.org/10.1016/j.firesaf.2021.103426

McGrattan K., Hostikka S., Floyd J., McDermott R., Vanella M., Mueller E., Fire Dynamics Simulator User's Guide, NIST Special Publication 1019, Sixth Edition, 2023 (April)

Merci, B., & Beji, T., Fluid Mechanics Aspects of Fire and Smoke Dynamics in Enclosures., 2016, CRC Press. https://doi.org/10.1201/9781003204374

Prétrel H., Saux W., Audouin L., Pressure variations induced by a pool fire in a well-confined and force-ventilated compartment, Fire Safety Journal, Volume 52, 2012, Pages 11-24, ISSN 0379-7112, https://doi.org/10.1016/j.firesaf.2012.04.005

Wahlqvist J., Hees P., Validation of FDS for large-scale well-confined mechanically ventilated fire scenarios with emphasis on predicting ventilation system behavior, Fire Safety Journal, Volume 62, Part B, 2013, Pages 102-114, ISSN 0379-7112, https://doi.org/10.1016/j.firesaf.2013.07.007

Annexure-A

Figure 11 shows the insensitivity of the pressure development on different roughness values.

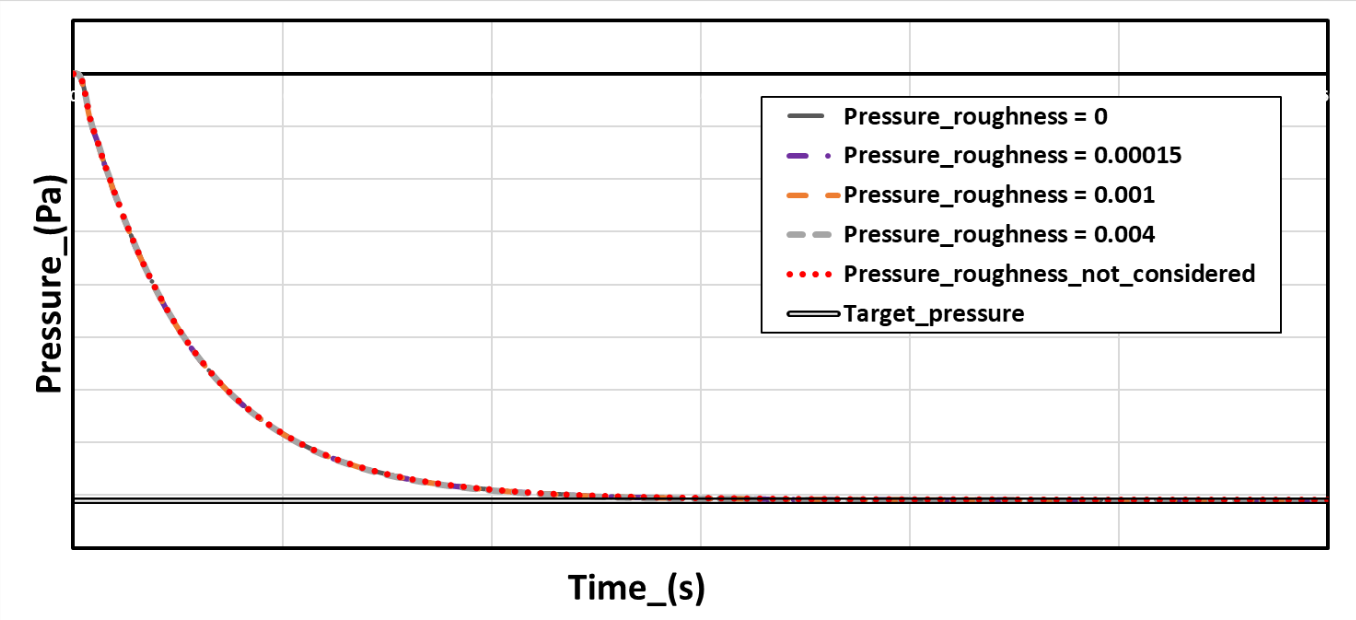

Figure 11. Effect of different roughness values on the establishment of the target pressure

DocuSign

Certificate Of Completion

Envelope Id: 3217D2070EA94468A74EDA8A0ED0B82D
Status: Completed
Subject: Complete with DocuSign: 6. VTT-ResearchReport (VTT-R-00784-23)_tyhja.pdf
Source Envelope:

Document Pages: 21	Signatures: 1	Envelope Originator:
Certificate Pages: 1	Initials: 0	Marko Mäkipää
AutoNav: Enabled		Tekniikantie 21, Espoo
EnvelopeId Stamping: Enabled		., . P.O Box1000, FI-0204
Time Zone: (UTC+02:00) Helsinki, Kyiv, Riga, Sofia, Tallinn, Vilnius		Marko.Makipaa@vtt.fi
		IP Address: 130.188.17.16

Record Tracking

Status: Original 07 December 2023 | 14:55	Holder: Marko Mäkipää Marko.Makipaa@vtt.fi	Location: DocuSign

Signer Events | Signature | Timestamp

Marko Mäkipää
marko.makipaa@vtt.fi
Research Team Leader
Teknologian tutkimuskeskus VTT Oy
Security Level: Email, Account Authentication (None), Digital Certificate

Signature Adoption: Pre-selected Style
Using IP Address: 130.188.17.16

Sent: 07 December 2023 | 14:57
Viewed: 07 December 2023 | 14:58
Signed: 07 December 2023 | 14:59

Signature Provider Details:

Signature Type: DocuSign Protect & Sign (Client ID: DDE5E85D-4085-40B6-8785-DA3CCD16D81E)

Signature Provider Location: https://ps-ws.dsf.docusign.net/ds-server/s/noauth/psm/tsp/sign

Signature Issuer: DocuSign Cloud Signing CA - SI1

Authentication: Access Code

Electronic Record and Signature Disclosure:
Not Offered via DocuSign

In Person Signer Events | Signature | Timestamp

Editor Delivery Events | Status | Timestamp

Agent Delivery Events | Status | Timestamp

Intermediary Delivery Events | Status | Timestamp

Certified Delivery Events | Status | Timestamp

Carbon Copy Events | Status | Timestamp

Witness Events | Signature | Timestamp

Notary Events | Signature | Timestamp

Envelope Summary Events

Envelope Summary Events	Status	Timestamps
Envelope Sent	Hashed/Encrypted	07 December 2023 | 14:57
Certified Delivered	Security Checked	07 December 2023 | 14:58
Signing Complete	Security Checked	07 December 2023 | 14:59
Completed	Security Checked	07 December 2023 | 14:59

Payment Events | Status | Timestamps